Applied Physics Letters

RESEARCH ARTICLE | MARCH 15 2021

Tunable asymmetric acoustic transmission via binary metasurface and zero-index metamaterials

Special Collection: Metastructures: From Physics to Application

Zhongming Gu; Xinsheng Fang; Tuo Liu; ... et. al

Appl. Phys. Lett. 118, 113501 (2021)
https://doi.org/10.1063/5.0046756

Applied Physics Letters ARTICLE scitation.org/journal/apl

Tunable asymmetric acoustic transmission via binary metasurface and zero-index metamaterials

Cite as: Appl. Phys. Lett. **118**, 113501 (2021); doi: 10.1063/5.0046756
Submitted: 6 February 2021 · Accepted: 26 February 2021 ·
Published Online: 15 March 2021

Zhongming Gu,[1,2] Xinsheng Fang,[3] Tuo Liu,[1,2] He Gao,[1,2] Shanjun Liang,[1,2] Yong Li,[3,a)] Bin Liang,[4,a)] Jianchun Cheng,[4] and Jie Zhu[1,2,a)]

AFFILIATIONS

[1]The Hong Kong Polytechnic University Shenzhen Research Institute, Shenzhen 518057, People's Republic of China
[2]Research Center for Fluid-Structure Interactions, Department of Mechanical Engineering, The Hong Kong Polytechnic University, Hung Hom, Kowloon, Hong Kong
[3]Institute of Acoustics, School of Physics Science and Engineering, Tongji University, Shanghai 200092, People's Republic of China
[4] Key Laboratory of Modern Acoustics, MOE, Institute of Acoustics, Department of Physics, Nanjing University, Nanjing 210093, People's Republic of China

Note: This Paper is part of the APL Special Collection on Metastructures: From Physics to Applications.
[a)]**Authors to whom correspondence should be addressed:** yongli@tongji.edu.cn; liangbin@nju.edu.cn; jiezhu@polyu.edu.hk

ABSTRACT

The pursuit of tunable asymmetric sound transmission has been a long-term topic since it could contribute to providing more flexibilities in many areas of acoustic engineering. The interference effect can be a feasible approach in which two waves with the same frequency superposed to form the resultant wave with manipulated amplitude according to the relative phase difference between them. However, strictly speaking, restricted by the spatial variance of phase, the manipulated domain created by the specific phase difference is always limited to a spot with dimensions much smaller than the wavelength. Here, we proposed a design to break this barrier that can realize the tunable asymmetric transmission via the combination of zero-index metamaterials and the binary metasurface. The zero-index metamaterial can provide the effective extremely large speed to shrink the infinite domain into a spot acoustically and the binary metasurface can be used to tune the specific phase difference. Numerical simulations and experimental measurements have good agreement and show that the acoustic waves impinged from the side of metasurface will be manipulated to have controllable transmission, while the acoustic waves impinged from the side of zero-index metamaterials will keep a high transmission. We think the proposed design is full of physical significance, which may find potential applications in many fields, like noise cancelation, acoustic imaging, and ultrasound therapy.

Zero-index media (ZIMs), characterized by effective infinite phase velocity, have attracted on-going attention and interest of researchers owing to their fascinating abilities in the wave manipulations that cannot be achieved naturally.[1–10] As the refractive index approaches zero approximately, the critical angle at the interface between air and ZIM will decline toward zero. It indicates that only normally incident waves can penetrate through ZIM.[8] Meanwhile, due to the infinite phase velocity, waves propagating inside the ZIM undergo no phase variation and keep a constant. These marvelous properties can be utilized to achieve many intriguing wave phenomena, such as super-coupling,[4] cloaking,[11] and asymmetric transmission.[6,8]

A metasurface, which is a new type of engineered functional material with planar and thin features, has been widely utilized to manipulate the wave propagation.[12–20] By tailoring the phase response of the building block judiciously, the arbitrary manipulations on the reflection and refraction can be achieved in many wave systems, such as optics,[21] acoustics,[22] and elastic waves.[23] A well-tailored metasurface is a flexible tool for the purpose of changing the wave vector of the transmitted waves. Recently, by combining the advantages of ZIM and metasurfaces, their integration has been proposed to manipulate the wave transmission with additional functionalities.[24–26] In principle, ZIMs can decouple the spatial-temporal relationship to have a quasi-invariant phase distribution yet metasurfaces can generate accurate phase control by adjusting their geometries. It may give rise to more possibilities and freedom to realize the extraordinary and complex wave manipulations by ingenious integrations of ZIMs and metasurfaces.

In this Letter, we present a unique design consisting of ZIM and binary metasurfaces to achieve tunable asymmetric wave

transmission[27–34] based on the ZIM enabled interference effect. In our approach, the ZIM is arranged in a waveguide and clamped by the hard boundary; meanwhile, two ports remain for the incidence and the transmittance. One port is covered by the binary metasurfaces and the other is connected to the background media. The binary metasurfaces contain two kinds of designed units to provide relative differences of phase response. The ZIM offers the generalized interference effect that mixes different incident waves linearly based on the quasi-invariant phase. In this way, by changing the filling ratio between the binary metasurfaces, the traveling wave impinged on the metasurface could have a tunable transmission coefficient. On the contrary, the beam impinged on the ZIM first will be confronted with the tunneling effect and remain intact. After that, the transmitted wave will have a slightly distorted wavefront imposed by the metasurface but still has high transmission efficiency. It should be noted that we employ the acoustic wave as the specific physical realization of our scheme here, but it can be easily extended to the fields of electromagnetic waves or optics, as they obey similar mathematical formulas.

As one of the most basic and important wave phenomena, the interference effect can be observed in all types of waves and plays a key role in acoustic engineering, including ultrasound imaging, active noise control, music instruments, and so on. Conventionally, multiple sinusoidal waves with the same amplitude and frequency can create the interference area constructively or destructively determined by the constant phase difference between them, which is governed by the superposition principle. Notably, when the phase difference is π, the interference area is tranquil and invariant spatially and temporally, which constitutes the fundamental basis of the active noise control.[35] However, restricted by the fact that the phase distribution varies along propagation path, the interference area may contain several constructive and destructive parts simultaneously and consequently turns out to be fringe patterns. Zooming in the patterns, the invariant spot still can be observed but with the dimension much smaller than the wavelength. After leaving away from the interference area, the incident waves keep unchanged and propagate independently. As the ZIM has the ability that enforces the large domain in reality to behave as a spot acoustically,[3] the process of wave interference in the ZIM may be different from the case in free space. Consider the ZIM is enclosed by the rigid boundary but leaves several ports for wave interaction. The multiple traveling waves incident normally can penetrate the ZIM and leave along the normal direction of the ports of the ZIM. As neither gain nor loss element has been taken into account in the ZIM, the net acoustic energy enclosed the ZIM should be 0, which can be expressed as follows:[36]

$$\sum_{k=1}^{n} I_k S_k = 0, \tag{1}$$

where I_k and S_k are the net acoustic intensity and size of the kth port, respectively. Equation (1) guarantees the continuity of acoustic energy flow across the ZIM and implies that both the incident waves and the sizes of ports contribute to the resultant waves. By combining the condition of pressure continuity, one may expect that the resultant waves can be controlled as designed by adjusting the incident waves and the sizes of the ports.

The ZIM-based interference effect also can be extended to the single beam that splits into two beams with different phases. Here, we consider a reduced model that the ZIM attached with the binary metasurface has been placed in the waveguide to have a verification, as shown in Fig. 1. The yellow and green areas that are separated by the rigid boundary are the binary metasurfaces that impose the incident waves with the additional phase responses φ_{add} and $\varphi_{\text{add}} + \Delta\varphi$, respectively. The blue area represents the ZIM that has the matched impedance with the background medium and near zero refractive index. The variable t is the filling ratio of the yellow area in the waveguide and $1 - t$ is the filling ratio of the green area accordingly. The traveling wave p_{i} incident from the left side will be divided into two parts by the binary metasurface with the additional phases: $p_{\text{i1}} = p_{\text{i}} \exp(i\varphi_{\text{add}})$ and $p_{\text{i2}} = p_{\text{i}} \exp(i\varphi_{\text{add}} + i\Delta\varphi)$, respectively. Moreover, the proportion of these two parts will be tuned by changing the filling ratio of t. It should be noted that the multiple reflections at the interfaces have been ignored for the sake of simplification. After superposing in the ZIM, the transmitted wave p_{t} can be deduced directly according to Eq. (1): $p_{\text{t}} = tp_{\text{i1}} + (1 - t)p_{\text{i2}}$. Subsequently, the acoustic pressure transmission coefficient can be written as follows:

$$T = e^{i\varphi_{\text{add}}}\left[t + (1 - t)e^{i\Delta\varphi}\right] \tag{2}$$

Equation (2) clearly shows that the absolute value of T is determined by the filling ratio t and phase difference $\Delta\varphi$. The transmission spectrum is mapped in Fig. 2(a) for an unambiguous explanation. The cases of $\Delta\varphi = 0$ and $\Delta\varphi = 2\pi$ indicate that there is no phase difference between the two kinds of metasurface units, which brings the transmission coefficient close to 1. Similarly, the cases of $t = 0$ and $t = 1$ indicate that only one kind of metasurface unit takes a dominant role, which also leads to nearly full transmission. However, the coefficient will approach zero at the specific case of $t = 1/2$ and $\Delta\varphi = \pi$ simultaneously owing to the fact that the two parts take the same proportion and opposite signs. The waves incident from the left side will be blocked and reflected totally under these conditions. The variances of t and $\Delta\varphi$ also have impacts on the phase spectrum, as mapped in Fig. 2(b). Apparently, in the case of $t = 0$, the phase response of the transmission coefficient will have a change as $\Delta\varphi$ varies from 0 to 2π. On the contrary, in the case of $t = 1$, the phase response will keep unchanged as the $\Delta\varphi$ has little influence on the transmitted wave. In particular, when $t = 1/2$ and $\Delta\varphi = \pi$, the phase response will reel from a shift of π as the dominant part changes. For the situation that the wave is incident from the right side, the propagation encounters a much simpler process. Owing to the tunneling effect, the incident

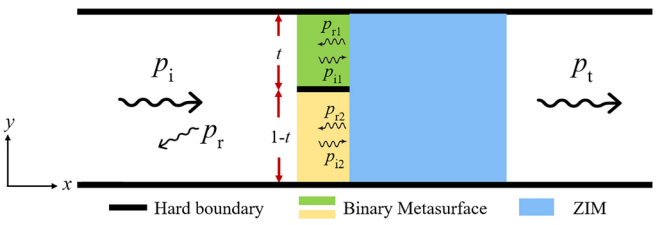

FIG. 1. Model for tunable transmission. The combination of the binary metasurface and ZIM is arranged in the waveguide covered by the rigid boundary. The yellow and green regions represent the metasurfaces with different phase responses; t and $1 - t$ are the filling ratios for them. The blue region represents the ZIM. p_{i} denotes the incident wave, which has been divided into two parts: p_{i1} and p_{i2} by the metasurface. p_{r1} and p_{r2} are the reflected waves generated at the interface. p_{r} and p_{t} denote the reflected and transmitted wave for the whole system.

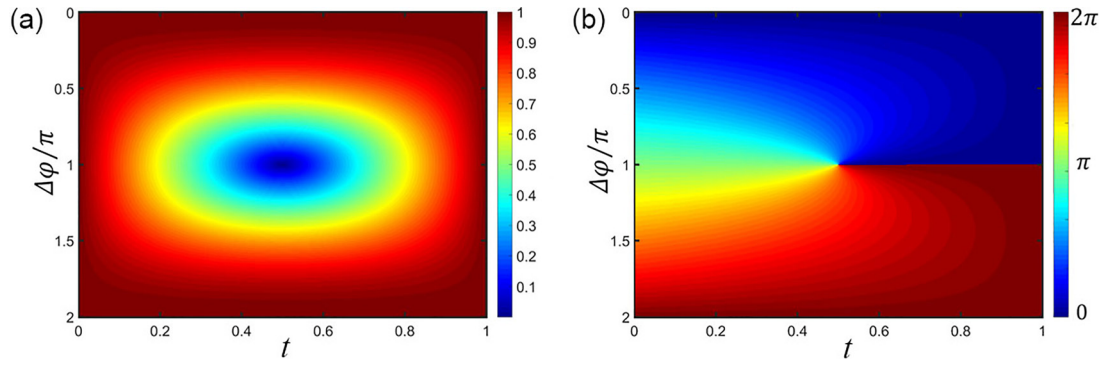

FIG. 2. The transmission properties. (a) Theoretically calculated amplitude of transmission coefficient responses to the phase difference $\Delta\varphi$ and filling ratio t. (b) Theoretically calculated phase of the transmission coefficient response to the phase difference $\Delta\varphi$ and filling ratio t.

wave will keep an intact wave-front and have a total transmission through the ZIM. In addition, the binary metasurface will have slight modulation on the transmitted wave and lead to a high energy transmission.

What needs to be emphasized is that, in the case of $\Delta\varphi = \pi$, the expression of the transmission coefficient will degenerate into $T = e^{i\varphi_{add}}(2t - 1)$. As the filling ratio of t is a real number, the amplitude and phase of the transmitted wave have been decoupled naturally.[19] On the one hand, the additional phase φ_{add} will be imposed upon the transmitted wave by the metasurface, which can be controlled as designed. On the other hand, the amplitude of the resultant wave will be modulated by altering the filling ratio t independently (see the supplementary material for the decoupled transmission amplitude and phase). Obviously, the φ_{add} can also be set as gradient values along the surface of the metasurface,[12] which can be applied to the case of oblique incidence (see the supplementary material for the case of oblique incidence).

To experimentally investigate the tunable and asymmetric transmission properties of the proposed model, we design and fabricate the sample with the help of a 3D printer, which is shown in Fig. 3(a). Here, we introduce the hybrid structures with 4 side-loaded Helmholtz resonators to act as the binary metasurface,[22] as enclosed by yellow (Type 1 units) and green (Type 2 units) dashed lines in Fig. 3(a), respectively. By adjusting the structural parameters of the units carefully, the phase response of the transmitted waves can be modulated in the range of 0 to 2π with high transmission (see the supplementary material for the detailed design of the units). These two types of units have been designed to have a π phase difference. 8 units with the same size have been arranged along the y axis to constitute the binary metasurface, and the filling ratio of certain type of units can be controlled easily by changing the number of units. We also employ the labyrinth-like structure[37] that preserves the matched impedance and effective near zero refractive index[38,39] to act as ZIM (see the supplementary material for the design of the units). A 4×4 ZIM array, enclosed by a blue dashed line in Fig. 3(a), is arranged to connect with the metasurface. The working frequency has been chosen as 2615 Hz, and the structure parameters of the model have been set as $a = 3$cm and $L = 6.5$cm to guarantee that the size of unit is much smaller than the wavelength. 8 2-in. loudspeakers are employed to form a speaker array to generate the plane wave, and the transmitted acoustic energy has been integrated at the output port. For the waves traveling along the x axis, the transmitted wave will be modulated by the sample according to the above discussion. To eliminate the doubt that thermoacoustic viscosity may ruin the transmission performance, first of all, the normalized pressure transmission spectra for the cases that the whole units constituted by Type 1 or Type 2 have been measured, as displayed in Fig. 3(b). Both Type 1 units and Type 2 units show the property of high transmission and the spectra have a similar profile that reaches sharp peaks around 2615 Hz owing to the tunneling effect of the ZIM. For a comparison, the ambient sound pressure has been measured in the situation without source excitation, which has been labeled as noise floor in Fig. 3(b). The profile reflects that there are

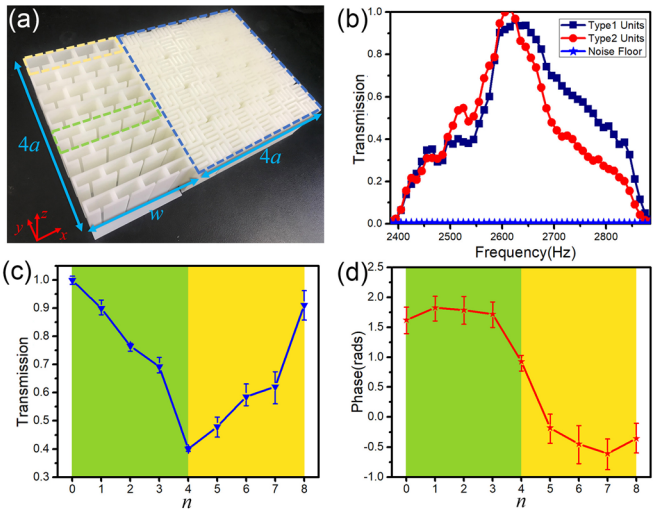

FIG. 3. Sample fabrication and demonstrations of tunable transmission. (a) Photograph of the fabricated sample for tunable asymmetric transmission, which consists of 8 metasurface units and the 4×4 labyrinth-like structure array. We define that the negative direction is along the x axis and positive direction is against the x axis contrarily. (b) The transmission spectra for the cases that the whole metasurface units are type 1 and type 2, respectively. The measured results have been normalized to the maximal value. The background noise floor has also been taken into account for a comparison. (c) The measured transmission amplitude vs the parameter of n. (d) The measured transmission phase vs the parameter of n.

clear transmitted waves despite the existence of thermoacoustic viscosity. Meanwhile, the transmission spectrum of the ZIM also restricts our model in a relatively narrow working bandwidth.

The process that replaces the metasurface units from type 2 to type 1 in sequence will introduce the variable of filling ratio t. In the practical realization, we use an integer n that indicates the number of type 1 units to represent the filling ratio since the metasurface has been discretized into 8 units. In the case that the whole units are type 2, n is 0. While changing the units from type 2 to type 1 one by one, n will increase to 8 gradually, which means all units are type 1. The transmission measurements for different n have been conducted for multiple times to obtain reliable averages, and the results have been normalized to maximal values. The pressure transmission spectrum displayed in Fig. 3(c) presents that the amplitudes of the transmitted waves indeed decrease monotonously with the increase in n and reach a dip when n is 4, as predicted by Eq. (2). After that, as n increases from 4 to 8 one by one, the spectrum profile will be reversed and approaches a high transmittance again. We further calculate the phase information of the transmitted waves according to the comparison with the excitation signals, as plotted in Fig. 3(d). The phase profile is separated into two parts by a shift at $n = 4$. Both the left part and the right part have the quasi-even line shapes that are determined by the dominant part being Type 2 or Type 1, respectively, and the gap between them equals the difference of the phase response between the Type 2 units and Type 1 units. During the theoretical calculations in Figs. 2(a) and 2(b), we assume that both the types of units that constitute the binary metasurface have the total transmission and rigorous phase difference as designed, which is hardly achievable at one take due to the existence of fabrication errors and acoustic loss. Both unequal transmission and the inaccurate phase response may harm the performance of the model and lead to imperfect results (see the supplementary material for the error analysis).

Finally, we demonstrate the asymmetric transmission realized by the integration of binary metasurfaces with ZIM, as illustrated in Fig. 4. Figures 4(a) and 4(d) show the simulated absolute pressure distributions when the acoustic waves impinged on both sides of the model, respectively, in which the green arrows represent the incident waves. The 2D full-wave numerical simulations are conducted by the finite element method with COMSOL Multiphysics (5.2a). As the rectification ratio is an important factor for asymmetric transmission, here, we consider $n = 4$ for the specific case since it has the lowest transmission along the negative direction, as shown in Fig. 4(a). The incident waves impinged on the metasurface are almost reflected and leave a silent area on the other side of the model. However, things changed totally in the case that the incident waves impinged on the ZIM first, as shown in Fig. 4(d). The slight fringes along the incident direction imply that minor standing waves are generated and most of the acoustic energy has transmitted through the structure. Figure 4(d) also points out that the transmitted waves along the positive direction have an irregular distribution since the wavefront has been modulated by the metasurface in a divergent way. In the measurement, the moving stage is utilized to support the 2D scanning. The measured regions ($12 \times 30\,\mathrm{cm}^2$) have been meshed into 330 measured points with a spacing of 1 cm (see the supplementary material for the experimental setup). Figures 4(b) and 4(c) show the measured absolute pressure fields when the traveling waves are incident along positive and negative directions, corresponding to the areas enclosed by the dashed lines in Figs. 4(d) and 4(a), respectively. Strong contrast between lights and shades can be observed by comparing the measured results in Figs. 4(b) and 4(c), which means that robust asymmetric transmission can be achieved by the proposed structure that the incident waves have an unencumbered transmission along the positive direction while being blocked and reflected totally along the opposite direction. Meanwhile, by changing the filling ratio of the binary units of the metasurface, the transmission along the negative direction can be modulated arbitrary, which may find potential applications in many areas of acoustic engineering.

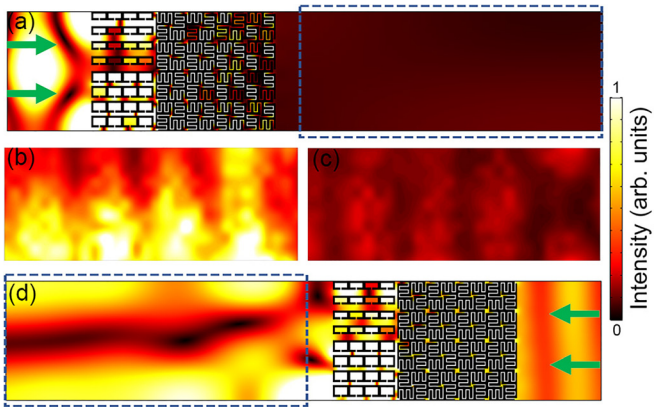

FIG. 4. Asymmetric transmission generated by the proposed model. (a) The simulated acoustic intensity distributions for the waves incident along the negative direction. The green arrows represent the incident waves. (b) The measured results for the area enclosed by the dashed line in (d). (c) The measured results for the area enclosed by the dashed line in (a). (d) The simulated acoustic intensity distributions for the waves incident along the positive direction.

In summary, we have proposed and demonstrated an acoustic metamaterial consisting of binary metasurfaces and zero-index metamaterials, which enables the tunable and asymmetric transmission that restrains the waves incident from the negative direction with a fully controlled transmission while allowing the waves incident from the positive direction travel through totally. The labyrinth-like structure has been employed to realize the impedance matched zero-index metamaterials that offers the capabilities to superpose the incident waves based on the pressure and volume flow continuities. The hybrid structure with 4 side-loaded Helmholtz resonators has been utilized to form the binary metasurfaces that divide the incident wave into two parts and impose the predesigned phase difference between them. By judiciously changing the phase difference and filling ratio of the binary metasurface, our design has been demonstrated both numerically and experimentally. The measured transmitted fields show a strong contrast between the waves incident from positive and negative directions, which implies the asymmetric transmission indeed occurs.

For the topic of asymmetric transmission, compared to previous schemes that can barely suppress the transmission along the negative direction, our scheme provides a versatile approach that could have significant applications in many areas, such as noise control, ultrasound imaging, and therapy. By decoupling the transmission amplitude and phase simultaneously, we envision that our findings may enrich the freedom to inspire more intriguing wave phenomena.

See the supplementary material for the details on the decoupled transmission amplitude and phase, the case for oblique incidence, the design of component units, the influence of the differences between the two units consisting of the binary metasurface, and the experimental setup.

This work was supported by the National Natural Science Foundation of China (Grant No. 11774297) and General Research Fund (GRF) scheme of Research Grants Council of Hong Kong (Grant No. PolyU 152119/18E).

DATA AVAILABILITY

The data that support the findings of this study are available from the corresponding author upon reasonable request.

REFERENCES

[1]I. Liberal, A. M. Mahmoud, Y. Li, B. Edwards, and N. Engheta, "Photonic doping of epsilon-near-zero media," Science **355**, 1058–1062 (2017).
[2]M. Dubois, C. Shi, X. Zhu, Y. Wang, and X. Zhang, "Observation of acoustic Dirac-like cone and double zero refractive index," Nat. Commun. **8**, 14871 (2017).
[3]A. M. Mahmoud and N. Engheta, "Wave-matter interactions in epsilon-and-mu-near-zero structures," Nat. Commun. **5**, 5638 (2014).
[4]R. Fleury and A. Alu, "Extraordinary sound transmission through density-near-zero ultranarrow channels," Phys. Rev. Lett. **111**, 055501 (2013).
[5]H. Ge, M. Yang, C. Ma, M.-H. Lu, Y.-F. Chen, N. Fang, and P. Sheng, "Breaking the barriers: Advances in acoustic functional materials," Natl. Sci. Rev. **5**, 159–182 (2018).
[6]Z-m Gu, B. Liang, X-y Zou, J. Yang, Y. Li, J. Yang, and J-c Cheng, "One-way acoustic mirror based on anisotropic zero-index media," Appl. Phys. Lett. **107**, 213503 (2015).
[7]Q. Wei, Y. Cheng, and X-J. Liu, "Acoustic total transmission and total reflection in zero-index metamaterials with defects," Appl. Phys. Lett. **102**, 174104 (2013).
[8]Y. Li, B. Liang, Z-m Gu, X-y Zou, and J-c Cheng, "Unidirectional acoustic transmission through a prism with near-zero refractive index," Appl. Phys. Lett. **103**, 053505 (2013).
[9]J. Luo, B. Liu, Z. H. Hang, and Y. Lai, "Coherent perfect absorption via photonic doping of zero-index media," Laser Photonics Rev. **12**, 1800001 (2018).
[10]Z. Gu, H. Gao, T. Liu, Y. Li, and J. Zhu, "Dopant-modulated sound transmission with zero index acoustic metamaterials," J. Acoust. Soc. Am. **148**, 1636 (2020).
[11]X.-F. Zhu, "Effective zero index in locally resonant acoustic material," Phys. Lett. A **377**, 1784–1787 (2013).
[12]N. Yu, P. Genevet, M. A. Kats, F. Aieta, J. P. Tetienne, F. Capasso, and Z. Gaburro, "Light propagation with phase discontinuities: Generalized laws of reflection and refraction," Science **334**, 333–337 (2011).
[13]B. Assouar, B. Liang, Y. Wu, Y. Li, J.-C. Cheng, and Y. Jing, "Acoustic metasurfaces," Nat. Rev. Mater. **3**, 460–472 (2018).
[14]S. A. Cummer, J. Christensen, and A. Alù, "Controlling sound with acoustic metamaterials," Nat. Rev. Mater. **1**, 16001 (2016).
[15]Y. Li, B. Liang, Z. M. Gu, X. Y. Zou, and J. C. Cheng, "Reflected wavefront manipulation based on ultrathin planar acoustic metasurfaces," Sci. Rep. **3**, 2546 (2013).
[16]J. Mei and Y. Wu, "Controllable transmission and total reflection through an impedance-matched acoustic metasurface," New J. Phys. **16**, 123007 (2014).
[17]J. Li, C. Shen, A. Diaz-Rubio, S. A. Tretyakov, and S. A. Cummer, "Systematic design and experimental demonstration of bianisotropic metasurfaces for scattering-free manipulation of acoustic wavefronts," Nat. Commun. **9**, 1342 (2018).
[18]Y. Xie, W. Wang, H. Chen, A. Konneker, B. I. Popa, and S. A. Cummer, "Wavefront modulation and subwavelength diffractive acoustics with an acoustic metasurface," Nat. Commun. **5**, 5553 (2014).
[19]Y. Tian, Q. Wei, Y. Cheng, and X. Liu, "Acoustic holography based on composite metasurface with decoupled modulation of phase and amplitude," Appl. Phys. Lett. **110**, 191901 (2017).
[20]Z. Tian, C. Shen, J. Li, E. Reit, Y. Gu, H. Fu, S. A. Cummer, and T. J. Huang, "Programmable acoustic metasurfaces," Adv. Funct. Mater. **29**, 1808489 (2019).
[21]N. Yu and F. Capasso, "Flat optics with designer metasurfaces," Nat. Mater. **13**, 139–150 (2014).
[22]Y. Li, X. Jiang, B. Liang, J-c Cheng, and L. Zhang, "Metascreen-based acoustic passive phased array," Phys. Rev. Appl. **4**, 024003 (2015).
[23]Y. Liu, Z. Liang, F. Liu, O. Diba, A. Lamb, and J. Li, "Source illusion devices for flexural lamb waves using elastic metasurfaces," Phys. Rev. Lett. **119**, 034301 (2017).
[24]H. Chu, Q. Li, B. Liu, J. Luo, S. Sun, Z. H. Hang, L. Zhou, and Y. Lai, "A hybrid invisibility cloak based on integration of transparent metasurfaces and zero-index materials," Light Sci. Appl. **7**, 50 (2018).
[25]C. Shen, Y. Xie, J. Li, S. A. Cummer, and Y. Jing, "Asymmetric acoustic transmission through near-zero-index and gradient-index metasurfaces," Appl. Phys. Lett. **108**, 223502 (2016).
[26]X. Jiang, B. Liang, J. Yang, J. Yang, and J-c Cheng, "Acoustic planar antireflective focusing lens with sub-diffraction-limit resolution based on metamaterials," J. Appl. Phys. **123**, 091717 (2018).
[27]B. Liang, B. Yuan, and J. C. Cheng, "Acoustic diode: Rectification of acoustic energy flux in one-dimensional systems," Phys. Rev. Lett. **103**, 104301 (2009).
[28]Y. Li, C. Shen, Y. Xie, J. Li, W. Wang, S. A. Cummer, and Y. Jing, "Tunable asymmetric transmission via lossy acoustic metasurfaces," Phys. Rev. Lett. **119**, 035501 (2017).
[29]B. I. Popa and S. A. Cummer, "Non-reciprocal and highly nonlinear active acoustic metamaterials," Nat. Commun. **5**, 3398 (2014).
[30]Z. M. Gu, J. Hu, B. Liang, X. Y. Zou, and J. C. Cheng, "Broadband non-reciprocal transmission of sound with invariant frequency," Sci. Rep. **6**, 19824 (2016).
[31]J. Zhu, X. Zhu, X. Yin, Y. Wang, and X. Zhang, "Unidirectional extraordinary sound transmission with mode-selective resonant materials," Phys. Rev. Appl. **13**, 041001 (2020).
[32]T. Liu, G. Ma, S. Liang, H. Gao, Z. Gu, S. An, and J. Zhu, "Single-sided acoustic beam splitting based on parity-time symmetry," Phys. Rev. B **102**, 014306 (2020).
[33]Y. Wang, J. P. Xia, H. X. Sun, S. Q. Yuan, Y. Ge, Q. R. Si, Y. J. Guan, and X. J. Liu, "Multifunctional asymmetric sound manipulations by a passive phased array prism," Phys. Rev. Appl. **12**, 024033 (2019).
[34]J. P. Xia, X. T. Zhang, H. X. Sun, S. Q. Yuan, J. Qian, and Y. Ge, "Broadband tunable acoustic asymmetric focusing lens from dual-layer metasurfaces," Phys. Rev. Appl. **10**, 014016 (2018).
[35]M. O. Tokhi, *Active Noise Control.* (Clarendon Press/Oxford University Press, Oxford/New York, 1992).
[36]P. M. Morse, *Theoretical Acoustics*. (McGraw-Hill, New York, 1968).
[37]Z. Liang and J. Li, "Extreme acoustic metamaterial by coiling up space," Phys. Rev. Lett. **108**, 114301 (2012).
[38]V. Fokin, M. Ambati, C. Sun, and X. Zhang, "Method for retrieving effective properties of locally resonant acoustic metamaterials," Phys. Rev. B **76**, 144302 (2007).
[39]H. Gao, X. Fang, Z. Gu, T. Liu, S. Liang, Y. Li, and J. Zhu, "Conformally mapped multifunctional acoustic metamaterial lens for spectral sound guiding and Talbot effect," Research **2019**, 1748537.